

Field dependence of the microwave resistivity in $\text{SmBa}_2\text{Cu}_3\text{O}_7$ thin films.

E. Silva^{(1)†}, N. Pompeo⁽¹⁾, L. Muzzi^{(1)‡}, R. Marcon⁽¹⁾, S. Sarti⁽²⁾, M. Boffa⁽³⁾, A. M. Cucolo⁽³⁾

⁽¹⁾ *Dipartimento di Fisica "E. Amaldi" and Unità INFM, Università di Roma Tre, Via della Vasca Navale 84, 00146 Roma, Italy*

⁽²⁾ *Dipartimento di Fisica and Unità INFM, Università "La Sapienza", 00185 Roma, Italy*

⁽³⁾ *Dipartimento di Fisica and Unità INFM, Università di Salerno, Baronissi, Salerno, Italy*
(preprint)

We report measurements of the microwave complex resistivity at 48 GHz in $\text{SmBa}_2\text{Cu}_3\text{O}_{7-\delta}$ thin films. Measurements are performed with a moderate magnetic field, $\mu_0 H < 0.8\text{T}$, applied along the c -axis. We find that the complex resistivity presents clear sublinear field dependences, and that the imaginary part is remarkably sensitive to the moderate magnetic field. Interpretation considering an unusually strong pinning leads to very anomalous field dependences of the single-vortex viscosity and of the pinning constant. By contrast, allowing for a significant effect of the magnetic field on the depletion of the condensate, the data are quantitatively described by the simple free-flow-like expression, supplemented with two-fluid conductivity. In this frame, we obtain the vortex viscosity from the data. We compare vortex viscosity in $\text{SmBa}_2\text{Cu}_3\text{O}_{7-\delta}$ and in $\text{YBa}_2\text{Cu}_3\text{O}_{7-\delta}$.

74.25.Nf, 74.60.Ec, 74.60.Ge, 74.72.Jt

I. INTRODUCTION

The microwave response is a source of important information in superconductors. In high- T_c superconductors (HTCS) various microwave techniques have been used to get information, among the others, on the symmetry of the order parameter, on the vortex parameters such as the vortex viscosity and pinning frequency^{2,3,1} and on the temperature dependence of the superfluid fraction (via the measurement of the temperature dependence of the London penetration depth⁴). In short, microwave measurements are a very powerful tool to study the superconducting state.

While $\text{YBa}_2\text{Cu}_3\text{O}_{7-\delta}$ (YBCO) and, to a minor extent, $\text{Bi}_2\text{Sr}_2\text{CaCu}_2\text{O}_{8+x}$ (BSCCO) have been the subject of intensive experimental investigation, other HTCS did not receive the same attention. In particular, a very few reports dealt with the vortex-state microwave response in rare-earth substituted 123 compounds, mainly on Dy⁵ and Gd-substituted materials.^{6,7} In fact, RE-substituted 123 compounds present potentially interesting features in the vortex state: in particular, they often give enhanced irreversibility lines⁸ and in some case a T_c slightly higher than in YBCO. To what extent those features can change the microwave properties in the vortex state is not known, nor it is clear what effect substitutions can have on the pinning at high frequencies. Aim of this paper is to present an extensive study of the microwave response of $\text{SmBa}_2\text{Cu}_3\text{O}_{7-\delta}$ (SmBCO) in the vortex state in moderate fields, up to the critical temperature. It will be shown that the complex resistivity shows up an unexpectedly

strong field dependence. In particular, the imaginary part increases noticeably with the applied magnetic field at low temperatures, becomes nearly field-independent at a sample-dependent temperature around $T/T_c \sim 0.9$ and then decreases with the application of the field up to T_c . In addition, both the real and imaginary parts of the resistivity present clear sublinear field dependences. We show that all those findings cannot be easily understood within the conventional framework for vortex motion at high frequencies. By contrast we find that, by assuming a significant effect of the magnetic field on the superfluid depletion, all the temperature and field dependences are well described by the simple viscous vortex motion supplemented with the two-fluid conductivity. We obtain almost the same temperature-dependent vortex viscosity in two different samples, in agreement with its intrinsic origin. Consistently, the temperature dependence of the vortex viscosity in SmBCO is identical to the one measured in YBCO.

II. SAMPLES PREPARATION AND EXPERIMENTAL RESULTS

The $\text{SmBa}_2\text{Cu}_3\text{O}_{7-\delta}$ films were deposited on (100)KLaAlO₃ substrates by a high oxygen pressure sputtering technique. Even if these substrates show higher mismatch in comparison with the SrTiO₃, the use of LaAlO₃ is mandatory for microwave studies and applications due to its low loss tangent. Sintered targets⁹ of 35 mm diameter and of 2 mm thickness were used. The nom-

[†]To whom correspondence should be addressed. E-mail: silva@fis.uniroma3.it

[‡]Present Address: ENEA, Frascati, Roma, Italy.

inal composition of the metal elements (Sm:Ba:Cu) in the targets was 1:2:3. All the films were deposited at high temperatures, with the substrates placed onto an inconel heater whose temperature was monitored by a thermocouple embedded into the furnace. The films were grown in a vacuum chamber at constant oxygen pressure P_{O_2} and substrate temperature T_d during the deposition. The tetragonal to orthorhombic phase transition was accomplished after the deposition process by cooling the samples in an oxygen pressure of one atmosphere from T_d to the annealing temperature, T_a , kept constant for the time of the annealing process, t_a . The samples were finally cooled down to the room temperature. The main deposition parameters are: $T_d = 910^\circ\text{C}$, $P_{O_2} = 2.6$ mbars, $T_a = 560^\circ\text{C}$, $t_a = 15$ min. The crystal structure of the films was examined by X-ray $\theta - 2\theta$ diffraction. The X-ray diffraction pattern showed that the growth of the film onto a LaAlO_3 substrate was single phased with preferential orientation along the c axis. The rocking curve of the (005) peak exhibits a typical full width at half maximum (FWHM) of less than 0.2° . The surface morphology of the films was observed by atomic force microscopy (AFM) at room temperature. 2D-nucleation growth was observed, and roughness was found to be ~ 2 nm on $1 \mu\text{m} \times 1 \mu\text{m}$ area. Film thickness was typically $d \approx 200$ nm. Two films were prepared, with $T_c \simeq 86.5$ K, as determined from the inflection point of the temperature-dependent real resistivity. The dc resistivity at 100 K was $\rho(100) \simeq 300 \mu\Omega\text{cm}$ in both samples. Further details on sample preparation and structural characterization have been reported elsewhere.¹⁰

The microwave response was measured by the end-wall cavity technique at 48.2 GHz with a moderate magnetic field applied along the c -axis. The maximum attainable field was $B \simeq \mu_0 H \leq 0.8$ T. Q factor and resonance frequency ν_0 were measured as a function of the magnetic field at various fixed temperatures in the range 60-90 K. From the field induced change of Q and ν_0 the field induced change of the effective surface impedance $\Delta Z_s^{eff} = Z_s^{eff}(H, T) - Z_s^{eff}(0, T)$ could be obtained.¹¹ Due to the small thickness of the film, the thin film approximation applies to the measurements,¹² so that $\Delta Z_s^{eff} = \Delta \tilde{\rho}/d = \Delta \rho_1/d + i\Delta \rho_2/d$, where $\tilde{\rho}$ is the complex resistivity. It must be stressed that the absolute value of $\tilde{\rho}$ is affected by errors in the evaluation of the geometrical factor and of the film thickness, and in the calibration of the cavity.^{13,14} The first two are eliminated and the third strongly reduced by working with the reduced complex resistivity change, $\Delta \tilde{r} = \Delta r_1 + i\Delta r_2 = \Delta \rho_1/\rho_0 + i\Delta \rho_2/\rho_0$, with $\rho_0 = \rho(100 \text{ K})$. In the following we will work with the reduced quantity, since (as it will be clear later) the absolute values will be useful only in the discussion of the details of the parameters.

We now present the main features of our data. Two samples were investigated, and both presented the same experimental behaviour. In the following, we focus on measurements taken more systematically in sample A. In Figures 1 and 2 we report the field-sweeps at several

temperatures for the real and imaginary parts. The real part, Δr_1 , increases with the field, with increasing amplitude up to a typical temperature $T_{max} \approx 82$ K (Figure 1a), above which the application of the field has a lower and lower effect by increasing the temperature (Figure 1b). The imaginary part, Δr_2 , increases with the field at lower temperatures, becomes approximately field independent at $T_0 \approx 80$ K and then starts to decrease with the field (Figure 2) above T_0 . The same features are observed in sample B, with $T_0 \approx 77$ K. Both Δr_1 and Δr_2 exhibit a sublinear behaviour with respect to the applied field. The explicit field dependences of Δr_1 and Δr_2 can be directly identified by replotting the same data of Figures 1 and 2 vs \sqrt{B} (Figures 3 and 4). It is immediately seen that $\Delta r_2 \propto \sqrt{B}$, while Δr_1 has an upward curvature. Within the experimental uncertainty, Δr_1 is the sum of a linear and a square-root term in the applied field. Summarizing, the full body of our data in SmBCO can be described by the empirical relations:

$$\Delta r_1 = b_1(T)B + a_1(T)\sqrt{B} \quad (1)$$

$$\Delta r_2 = a_2(T)\sqrt{B} \quad (2)$$

Interestingly, these field dependences do not vary, neither when Δr_2 changes from positive to negative, nor when the temperature raises so that the measurements cross the irreversibility line (by increasing the temperature from 65 K to T_c we certainly cross B_{irr}), nor when the temperature is raised above T_{max} . Only very close to T_c (approximately 1 K below, where strong fluctuational effects become predominant) the field dependences empirically found appear to slightly modify and the empirical equations above no longer describe the data very accurately. All the obtained coefficients in the two samples studied have the same behavior as a function of the temperature, as reported in Figure 5 for a_1 and a_2 and in Figure 6 for b_1 . This is a clear indication (a) against the relevance of pinning at our measuring frequency, and (b) in favour of some ‘‘intrinsic’’ origin for the behaviour of the resistivity in the mixed state.

Given the very clear field dependences of the complex resistivity, we search for a theoretical frame able to describe our data, taking into account that no features appear when crossing the irreversibility line. In the following Section we briefly summarize the reference frame that we adopt for the theoretical description of the microwave response in the vortex state.

III. THEORETICAL SUMMARY

In principle, the response of a superconductor in the mixed state is dictated by the motion of vortices and of charge carriers. The latter originates from superfluid as well as normal carriers, and field-induced changes of the quasiparticle (QP) density have a direct effect on both

the real and the imaginary part. A general frame that includes all those contributions is the Coffey-Clem (CC) theory¹⁵ (a very similar model has been independently derived by Brandt¹⁶), based on the assumption of the two-fluid conductivity and of a periodic vortex pinning potential.

The general CC expression, including vortex, superfluid and QP contributions, is rather complex. In particular, the combined effect of pinning and creep make even the vortex motion alone of difficult description. In order to clarify the role of pinning, we first focus the attention below the irreversibility line where its effect is maximum. In the latter case, the characteristic frequency for the vortex diffusion reduces to the pinning frequency $2\pi\nu_p = k_p/\eta$, where η is the vortex viscosity and k_p the pinning constant (Labusch parameter). The resulting expression for the microwave complex resistivity $\tilde{\rho} = \rho_1 + i\rho_2$ in the vortex state can be then cast in the form:

$$\rho_1 = \frac{1}{1 + \left(\frac{\sigma_R}{\sigma_I}\right)^2} \left[\rho_{ff} \frac{1 + \frac{\nu_p \sigma_R}{\nu \sigma_I}}{1 + \left(\frac{\nu_p}{\nu}\right)^2} + \frac{1}{\sigma_R} \left(\frac{\sigma_R}{\sigma_I}\right)^2 \right] \quad (3)$$

and

$$\rho_2 = \frac{1}{1 + \left(\frac{\sigma_R}{\sigma_I}\right)^2} \left[\rho_{ff} \frac{\frac{\nu_p}{\nu} - \frac{\sigma_R}{\sigma_I}}{1 + \left(\frac{\nu_p}{\nu}\right)^2} + \frac{1}{\sigma_I} \right] \quad (4)$$

Where ν is the measuring frequency, $\rho_{ff} = \Phi_0 B/\eta$ is the so-called flux-resistivity, and $\sigma_R - i\sigma_I$ is the complex conductivity in absence of motion of vortices. The latter is temperature, field and frequency dependent, and contains the contributions of superfluid and QP, through their fractional densities and the QP scattering time.

These expressions have been sometimes used for the analysis of the microwave response in the vortex state.² However, in most cases it was judged that the field-dependence of the QP and superfluid densities was negligible, and that at low enough temperatures $\sigma_I \gg \sigma_R$. Within these approximations, the Coffey-Clem (CC) prediction for the field-induced changes to the resistivity reduces to the well-known Gittleman-Rosenblum (GR) model¹⁷ (in the GR model the QP and superfluid contributions are not considered, so the response is described by the vortex motion alone):

$$\Delta\rho_1(B) = \rho_1(B) - \rho_1(B=0) = \frac{1}{1 + \left(\frac{\nu_p}{\nu}\right)^2} \rho_{ff} \quad (5)$$

and

$$\Delta\rho_2(B) = \rho_2(B) - \rho_2(B=0) = \frac{\frac{\nu_p}{\nu}}{1 + \left(\frac{\nu_p}{\nu}\right)^2} \rho_{ff} \quad (6)$$

The latter model was in fact extensively used for the analysis of the microwave resistivity or surface impedance (see Ref.² and references therein). When it is possible to apply this conventional analysis, the vortex parameters ν_p and ρ_{ff} can be easily obtained by inverting the

data through Equations 5,6. The vortex viscosity is calculated as $\eta = \Phi_0 B/\rho_{ff}$. Finally, the pinning constant comes from the definition of ν_p .

In the following Section, we discuss first our data below the irreversibility line in terms of the GR model, and then within the CC model allowing for the inclusion of a possibly relevant effect of the magnetic field on the QP and superfluid fractional densities. The emerging frame strongly points toward the latter interpretation.

IV. DISCUSSION

When discussing our data on SmBCO we are faced with two main experimental features: the field dependences of r_1 and r_2 , which are clearly sublinear, and the very relevant increase of the imaginary part in even moderate fields. Since the role of pinning reveals itself mostly on the imaginary part, one might be tempted to assign the strong field dependence of Δr_2 simply to a strong pinning. Within this quite conventional view, one would apply the GR model and, following the procedure explained in Section III, would obtain ν_p , η , k_p directly from the data. The result of the procedure is reported in Figure 7 for several temperatures. As can be seen, the so-obtained pinning frequency would be a very weak function of the applied field, in agreement with commonly reported dependences.² However, the viscosity η would present a clear increase with the field (approximately as $\sim \sqrt{B}$), as reported in Figure 7 (panel b). This dependence is not easily explained. In fact, a similar behaviour at high fields has been tentatively explained in Bi₂Sr₂CuO₆ (Ref.¹⁸) in terms of a peculiar field dependence of the quasiparticle relaxation time in a d-wave superconductor, appearing when the intervortex distance becomes smaller than the mean free path. However, the model would explicitly predict the usual *field independence* at low fields. Due to our field and temperature ranges (by far lower than the temperature-dependent upper critical field), this picture does not seem very convincing. The anomalies become even more evident when, within the same GR model, we try to obtain the pinning constant k_p from the vortex pinning frequency and the vortex viscosity: as reported in Figure 7 (panel c), the so-obtained pinning constant would *increase* with the field (again, approximately as a square root). This behaviour does not seem reasonable. In particular, we note that in Ref.¹⁸ k_p was found to be constant at low fields, and to decrease at higher fields, as expected in high-frequency measurements. We conclude that an explanation of our data in terms of the GR model is at least questionable. We now show that the empirical field dependences for the complex resistivity can be immediately derived within a CC-like model, by including a field dependence of the QP fractional density in agreement with the existence of lines of nodes in the superconducting gap.

We first critically discuss the assumptions underlying the

CC model. The first assumption, the applicability of the two-fluid model, is reasonably justified by comparison with microwave studies^{19,20} of YBCO, which is the superconducting cuprate most similar to SmBCO. In particular, the imaginary part of the conductivity can be written as: $\sigma_I(T, B = 0) = \frac{x_{s0}(T)}{2\pi\nu\mu_0\lambda_0^2} \equiv \sigma_{I0}x_{s0}(T)$, where λ_0 is the zero-temperature London penetration depth, and x_{s0} is the temperature-dependent superfluid fraction, which is found²⁰ to be $x_{s0} \propto 1 - t^2$, with $t = T/T_c$, to a good approximation in the full temperature range from low temperatures up to very close to T_c . Moreover, it was found that the normal fluid fractional density x_{n0} decreased with decreasing temperature below T_c . In addition, no significant frequency dependence was observed²¹ in the real conductivity up to 75 GHz for temperatures $T > 60$ K indicating that at 50 GHz and above $T/T_c > \frac{2}{3}$ the real part of the conductivity can be written as $\sigma_R(T, B = 0) = \frac{ne^2\tau}{m}x_{n0}(T) \equiv \sigma_{R0}x_{n0}(T)$, where τ is the quasiparticle relaxation time.

Regarding the chosen description of the vortex motion, the assumption of periodic pinning potential is believed not to strongly affect the main features of the response, until the probing frequency is high enough to displace the vortices a small fraction of the intervortex distance, as is the case at high microwave frequencies. In fact, swept-frequency Corbino disk measurements in the frequency range 6-20 GHz³⁴ have shown that the frequency dependence of $\Delta\rho_1$ was well described by the Coffey-Clem expression for vortex dissipation, and gave estimates of the pinning frequency $(\nu_p/\nu)^2 \sim 5 \times 10^{-2}$ at 50 GHz and above 60 K.³⁵

Assuming that the main features of YBCO apply also to the closely related compound SmBCO, we compare our data to a CC-like model where the field-induced superfluid depletion is explicitly included, and we assume $\nu_p/\nu \ll 1$. The latter assumption is further supported by the experimental fact that our data do not show any detectable feature with increasing temperature from below to above the irreversibility line. In addition, at small enough fields, not too close to T_c we have $\rho_{ff}\sigma_R \ll 1$ and $\frac{\sigma_R}{\sigma_I} < 1$, so that Eq.s 3,4 simplify considerably and we obtain the approximate expressions:

$$\rho_1 \simeq \frac{\rho_{ff}}{1 + (\frac{\sigma_R}{\sigma_I})^2} + \frac{1}{\sigma_R} \frac{(\frac{\sigma_R}{\sigma_I})^2}{1 + (\frac{\sigma_R}{\sigma_I})^2} \quad (7)$$

and

$$\rho_2 \simeq \frac{1}{\sigma_I} \frac{1}{1 + (\frac{\sigma_R}{\sigma_I})^2} \quad (8)$$

It can also be shown that, within the approximations described above, Eq.s 7,8 remain valid above and below the irreversibility line: these approximate equations represent (a) the microwave response as given by free oscillations of flux lines (analytically described by the flux flow resistivity), given by the first term in Eq.7, and (b) the contribution from superfluid and QP conductivity, as

given by Eq.8 and by the second term in Eq.7.

An explicit field dependence of the two-fluid conductivity has to be inserted in these equations in order to compare them to the data. In a clean, conventional s-wave superconductor the superfluid density in the mixed state would decrease, and the QP fraction would increase, due to the density of states in the vortex cores. The effect would be proportional to the number of vortices, thus linear in B . However, it has been shown that in a superconductor with lines of nodes in the superconducting gap delocalized states (outside of the vortex cores) give a very significant contribution, exhibiting finite density of states at the Fermi level.^{27,30,29} The DOS is proportional to the number of vortices and to the spacing between them, thus leading to $x_n \sim \sqrt{B}$ increase of the QP fractional density. This effect has been experimentally observed in the specific heat of YBCO,²⁸ and in measurements of the QP fractional increase with sub-TeraHertz spectroscopy in BSCCO thin films.²⁵

We then incorporate the field dependence in the two-fluid conductivity through the superfluid and QP fractional densities³¹ as $x_s(T, B) = x_{s0}(T)(1 - b^\alpha)$ and $x_n(T, B) = 1 - (1 - x_{n0}(T))(1 - b^\alpha)$, with $b = B/cB_{c2}(T)$, $c \sim o(1)$ (Ref.³⁰) and $\alpha = \frac{1}{2}$ as appropriate for a superconductor with lines of nodes in the superconducting gap.^{25,27,30} Interestingly, taking into account that b^α is a small parameter, one can expand the two-fluid terms in Eq.s 7 and 8. One finally gets for the field variations of the normalized resistivity:

$$\begin{aligned} \Delta r_1(B) &\simeq \frac{1}{1 + S^2} \frac{\Phi_0}{\eta\rho_0} B + \frac{1}{\sigma_{R0}\rho_0} \frac{1}{x_{n0}} \frac{S^2}{(1 + S^2)^2} \times \\ &\times \left[1 + \frac{x_{s0}}{x_{n0}} + S^2 \left(1 - \frac{x_{s0}}{x_{n0}} \right) \right] \left(\frac{B}{cB_{c2}} \right)^{\frac{1}{2}} \\ &\equiv b_1(T)B + a_1(T)B^{\frac{1}{2}} \quad (9) \end{aligned}$$

and

$$\begin{aligned} \Delta r_2(B) &\simeq \frac{1}{\sigma_{R0}\rho_0} \frac{1}{x_{n0}} \frac{S}{(1 + S^2)^2} \left[1 - S^2 \left(1 + 2\frac{x_{s0}}{x_{n0}} \right) \right] \left(\frac{B}{cB_{c2}} \right)^{\frac{1}{2}} \\ &\equiv a_2(T)B^{\frac{1}{2}} \quad (10) \end{aligned}$$

where we have defined $S = \frac{\sigma_{R0}}{\sigma_{I0}} \frac{x_{n0}}{x_{s0}} \equiv S_0 \frac{x_{n0}}{x_{s0}}$. These two equations give exactly the functional field dependences that have been empirically found in the data. This is one of the main results of this paper: the experimental field dependence of the complex resistivity, not explainable in the framework of fluxon motion alone, is recovered by a model that includes simple free flux line oscillation (corresponding to flux flow resistivity) and the essential role of superfluid depletion in a superconductor with lines of nodes in the gap. We note that the inclusion of a vortex motion term in the imaginary resistivity would have given an additional *linear* term in Eq.10. To a great accuracy, no B -linear term is observed in the data, giving

further consistency to the approximations used to derive Eq.s 9,10. As a further relevant result, we note that the a_1 and a_2 coefficients here defined present the same qualitative features as in the experimental values: on one side, the study of Eq.9 reveals that a_1 can present a peak; more important, it is immediately seen that a_2 undergoes a sign change at a temperature such that:

$$S_0 = \left[\frac{x_{n0}}{x_{s0}} \left(2 + \frac{x_{n0}}{x_{s0}} \right) \right]^{-\frac{1}{2}} \quad (11)$$

Summarizing, the model here developed contains all the experimental features present in the data: the field dependences of the complex resistivity and the behavior with the temperature of a_1 and a_2 .

For a quantitative fit of the data with the theoretical expressions, one has to determine the temperature dependences of the parameters contained in Eq.s 9,10. Exploiting the similarities with YBCO, and consistently with the indication of the existence of lines of nodes in the gap, we have taken $x_{s0} = (1 - t^2)$ and $x_{n0} = t^2$, and $B_{c2} = B_{c20} (1 - t^2)$. To our knowledge there are no detailed studies of the finite frequency conductivity in SmBCO that could give indications on the temperature dependence of the QP scattering time: we then make the very crude assumption that the QP scattering time does not change much from above to below T_c . With this choice, one can write (apart small corrections due to the temperature dependence of the normal state resistivity, that we neglect here) $\sigma_{r0}\rho_0 \simeq 1$, and $S_0 \simeq const$. With this choice, on the basis of the constraint given by Eq.11 we have $S_0 = 0.146$ and 0.212 , in sample A and B, respectively.³⁷ The simultaneous fits of $a_1(T)$ and $a_2(T)$ contain only cB_{c20} as a common scale factor. In Figure 5 we plot the coefficients a_1 and a_2 , compared with the theoretical curves computed on the basis of Eq.s 9,10 with $cB_{c20} = 330$ T and 230 T as scale factors for sample A and B, respectively. The numerical values of S_0 are larger by a factor ~ 30 than expected with $\rho_0 \simeq 280 \mu\Omega\text{cm}$ and $\lambda_0 \sim 2000\text{\AA}$. Neglected effects, such that a temperature dependent quasiparticle scattering time,²⁰ a zero-temperature superfluid fraction less than unity, a two-component order parameter³⁸ might be responsible for this enhancement. Nevertheless, given the crudeness of the model and the absence of fit parameters, the theoretical expectations describe with surprising accuracy our data. We believe that the essential physics of the field dependent microwave response is related to the effects extensively described in this paper.

Finally, we discuss the fluxon dynamics. Within the present interpretation, it is entirely described by the coefficient b_1 . Using for $S = S_0 \frac{x_{n0}}{x_{s0}}$ the determinations obtained from a_1 and a_2 above, we immediately get the fluxon viscosity η , as reported in Figure 6. As can be seen, the data for η attain the same value in both samples, indicating that the physics in the vortex core is related to sample-independent processes.

Further insights can be gained by examining the data

within the Bardeen-Stephen model for the viscosity:³⁶ in this case $\eta = \Phi_0 B_{c2} / \rho_n$. Since (within 10%) ρ_n is the same in both samples, we deduce that also the upper critical field is the same. From that, we get for the constant c the relation $c_A/c_B \simeq 1.44$ (subscripts refer to the sample). Comparison with vortex viscosity data taken in YBCO³⁹ shows that: (a) the temperature dependence is the same in SmBCO and YBCO (minor differences appear only close to the critical temperature), and (b) the data of YBCO scale with a factor of 2 on the corresponding data in SmBCO, as we show in Figure 8. Since the ratio of the normal state resistivities at 100 K in the YBCO sample here reported and in the SmBCO samples is $\rho_0(\text{SmBCO})/\rho_0(\text{YBCO}) \simeq 3$, and $B_{c20}(\text{YBCO}) \simeq 165$ T,³³ using again the Bardeen-Stephen model we obtain $B_{c20}(\text{SmBCO}) \simeq 250$ T, $c_A \simeq 1.32$, $c_B \simeq 0.92$, in agreement with the requirement $c \sim o(1)$. It should be also noted that the vortex viscosities measured in YBCO are in excellent agreement⁴⁰ with those measured in YBCO crystals at three different frequencies,³ suggesting a common behavior for the electronic states in the vortex cores of SmBCO films, YBCO films and YBCO crystals.

As a final remark, we remind that the quantitative description of the vortex state microwave response here presented could be accomplished only with the essential inclusion of the enhanced QP increase in a magnetic field. A description in terms of fluxon motion alone would have given very unlikely dependences of the vortex parameters.

V. CONCLUSION

We have presented the first extensive vortex-state microwave characterization in SmBa₂Cu₃O_{7- δ} thin films as a function of the temperature and magnetic field. The field-dependence of the 48 GHz complex resistivity exhibits a markedly sublinear behaviour. The analysis in terms of strong pinning with weak field dependent superfluid depletion leads to internal contradictions, so that alternative interpretations have to be found. The experimental results give clear indications of the irrelevance of pinning at our measuring frequency. A framework including free oscillation of flux lines (whose resistivity is given by the flux flow expression) and an enhanced role of the field-induced pair breaking, due to the existence of lines of nodes in the superconducting gap, is able to describe the data qualitatively and quantitatively. The temperature dependences of the QP and superfluid contributions to the complex resistivity are fitted by the model with no free parameters. Within this frame, we estimate the fluxon viscosity and we find the same values in both SmBCO samples. The temperature dependence is the same as that measured in YBCO. Moreover, the viscosity data in SmBCO and YBCO scale together with a numerical factor. Using the Bardeen-Stephen model we estimate the upper critical field in SmBCO and the c constants,

which we consistently find $\sim o(1)$. We conclude that the vortex state resistivity in SmBCO is well described by vortex motion (that at our measuring frequencies takes the form of flux flow), with the essential contribution of the strong field dependence of the QP and superfluid fractional densities. The latter is connected to the structure of the superconducting gap.

ACKNOWLEDGEMENTS

Useful discussions with A. Maeda and R. Wördenweber are warmly acknowledged. Support from the ESF “VORTEX” program is acknowledged. This work has been partially supported by Italian MIUR under FIRB “Strutture semiconduttore/superconduttore per l’elettronica integrata”. L.M. acknowledges financial support from MIUR under the same project.

-
- ¹ J. Owliaei, S. Sridhar and J. Talvacchio, *Phys. Rev. Lett.* **69**, 3366 (1992)
- ² M. Golosovsky, M. Tsindlekht, D. Davidov, *Supercond. Sci. Technol.* **9**, 1 (1996), and references therein
- ³ Y. Tsuchiya, K. Iwaya, K. Kinoshita, T. Hanaguri, H. Kitano, A. Maeda, K. Shibata, T. Nishizaki, and N. Kobayashi, *Phys. Rev. B* **63**, 184517 (2001).
- ⁴ W.N. Hardy, D.A. Bonn, D.C. Morgan, R. Liang, K. Zhang, *Phys. Rev. Lett.* **70**, 3999 (1993).
- ⁵ A. R. Bhangale, P. Raychaudhuri, S. Sarkar, T. Banerjee, S. S. Bhagwat, V. S. Shirodkar, R. Pinto, *Phys. Rev. B* **63**, 180502 (2001)
- ⁶ H.A. Blackstead, D.B. Pulling, C.A. Clough, *Phys. Rev. B* **47**, 8978 (1993)
- ⁷ E. Silva, R. Marcon and F.C. Matarotta *Physica C* **218**, 109 (1993)
- ⁸ M. Murakami, N. Sakai, T. Higuchi, S.I. Yoo, *Supercond. Sci. Technol.* **9**, 1015 (1996); H. Kupfer, Th. Wolf, A.A. Zhukov, R. Meier-Hirmer, *Phys. Rev. B* **60**, 7631 (1999)
- ⁹ Produced by Hitec Materials.
- ¹⁰ C. Beneduce, F. Bobba, M. Boffa, A.M. Cucolo, M.C. Cucolo, A. Andreone, C. Aruta, M. Iavarone, F. Palomba, G. Pica, M. Salluzzo, R. Vaglio, *Int. J. Mod. Phys. B* **13**, 1333 (1999); M.A. Boffa, F. Bobba, A.M. Cucolo, R. Monaco, *Int. J. Mod. Phys. B* **17**, 768 (2003); M. Boffa, M.C. Cucolo, R. Monaco, A.M. Cucolo, *Physica C* **384**, 419 (2003).
- ¹¹ E. Silva, A. Lezzerini, M. Lanucara, S. Sarti and R. Marcon, *Meas. Sci. Technol.* **9**, 275 (1998)
- ¹² E. Silva, M. Lanucara, R. Marcon, *Supercond. Sci. Technol.* **9**, 934 (1996); N. Pompeo, R. Marcon and E. Silva, *Proceedings of 6th European Conference on Applied Superconductivity - EUCAS 2003*, 14-18/9/2003, Sorrento (Italy), to be published, paper 709.
- ¹³ J. Mazierska, *J. Supercond.* **10**, 73 (1997)
- ¹⁴ E. Silva, in *Superconducting Materials: Advances in Technology and Applications*, ed by A. Tampieri and G. Celotti, World Scientific, pp. 279-306 (2000), and references therein.
- ¹⁵ M.W. Coffey and J.R. Clem, *Phys. Rev. Lett.* **67**, 386 (1991)
- ¹⁶ H. Brandt, *Phys. Rev. Lett.* **67**, 2219 (1991)
- ¹⁷ J. I. Gittleman and B. Rosenblum, *Phys. Rev. Lett.* **16**, 734 (1966)
- ¹⁸ Y. Matsuda, A. Shibata, K. Izawa, H. Ikuta, M. Hasegawa, Y. Kato, *Phys. Rev. B* **66**, 014527 (2002)
- ¹⁹ D.A. Bonn, P. Dosanjh, R. Liang and W.N. Hardy, *Phys. Rev. Lett.* **68**, 2390 (1992).
- ²⁰ D.A. Bonn, R. Liang, T.M. Riseman, D.J. Baar, D.C. Morgan, K. Zhang, P. Dosanjh, T.L. Duty, A. MacFarlane, G.D. Morris, J.H. Brewer, W.N. Hardy, C. Kallin, A.J. Berlinsky, *Phys. Rev. B* **47**, 11314 (1993).
- ²¹ A. Hosseini, R. Harris, S. Kamal, P. Dosanjh, J. Preston, R. Liang, W.N. Hardy, D.A. Bonn, *Phys. Rev. B* **60**, 1349 (1999).
- ²² F. Gao, G.L. Carr, C.D. Porter, D.B. Tanner, G.P. Williams, C.J. Hirschmugl, B. Dutta, X.D. Wu, S. Etamad, *Phys. Rev. B* **54**, 700 (1996).
- ²³ J. Corson, R. Mallozzi, J. Orenstein, J.N. Eckstein and I. Bozovic *Nature* **398**, 221 (1999).
- ²⁴ J. Corson, J. Orenstein, J.N. Eckstein and I. Bozovic *Phys. Rev. Lett.* **81**, 1485 (1998).
- ²⁵ R. Mallozzi, J. Orenstein, S. Oh, J. O’Donnell, J.N. Eckstein, *Phys. Rev. Lett.* **85**, 2569 (2000).
- ²⁶ B. Parks, S. Spielman, J. Orenstein, D.T. Nemeth, F. Ludwig, J. Clarke, P. Marchant, and D.J. Lew, *Phys. Rev. Lett.* **74**, 3265 (1995).
- ²⁷ G.E. Volovik, *JETP Lett.* **58**, 469 (1993)
- ²⁸ K.A. Moler, D.J. Baar, J.S. Urbach, R. Liang, W.N. Hardy and A.K. Kapitulnik, *Phys. Rev. Lett.* **73**, 2744 (1994).
- ²⁹ S.K. Yip and J.A. Sauls, *Phys. Rev. Lett.* **69**, 2264 (1992).
- ³⁰ H. Won and K. Maki, *Phys. Rev. B* **53**, 5927 (1996).
- ³¹ We have taken for simplicity a field-independent quasiparticle scattering time. However, it is easy to show that this choice changes the subsequent equations only by some numerical factor. For example, allowing for an electron-vortex scattering like the one proposed in³², one would only redefine the quantity $\frac{x_s}{x_n}$ in Eq.s9,10.
- ³² M. Ausloos, *Supercond. Sci. Technol.* **12**, 11 (1999)
- ³³ E. Silva, R. Fastampa, M. Giura, R. Marcon, D. Neri and S. Sarti, *Supercond. Sci. Technol.* **13** 1186 (2000); R. Rogai, R. Marcon, E. Silva, R. Fastampa, M. Giura, S. Sarti, M. Boffa, A.M. Cucolo, *Int. J. Mod. Phys. B* **14**, 2828 (2000)
- ³⁴ S. Sarti, C. Amabile, N. Tosoratti, E. Silva, condmat/0307143; C. Amabile, R. Fastampa, M. Giura, S. Sarti, E. Silva, V. Ferrando, C. Ferdeghini, *Proceedings of 6th European Conference on Applied Superconductivity - EUCAS 2003*, 14-18/9/2003, Sorrento (Italy), to be published.
- ³⁵ S. Sarti, C. Amabile, R. Fastampa, M. Giura, E. Silva, *Proceedings of 6th European Conference on Applied Superconductivity - EUCAS 2003*, 14-18/9/2003, Sorrento (Italy), to be published.
- ³⁶ J. Bardeen and M.J. Stephen, *Phys. Rev. B* **140**, A1197 (1965).
- ³⁷ With a different choice of the temperature dependence of x_{n0} and x_{s0} one would have different S_0 . As an example, in sample A we have tried $x_{n0} = t^\alpha$ and $x_{s0} = 1 - x_{n0}$, with

$\alpha = 1, 2, 4$ (and correspondingly $S_0 = 0.075, 0.146, 0.278$ for our values of T_0), obtaining nearly identical fits (with the same scale factor).

³⁸ H. Srikanth, B. A. Willemsen, T. Jacobs, S. Sridhar, A. Erb, E. Walker, and R. Flükiger *Phys. Rev. B* **55**, R14733 (1997); H. Srikanth, Z. Zhai, S. Sridhar, A. Erb, and E. Walker *Phys. Rev. B* **57**, 7986 (1998)

³⁹ E. Silva, R. Marcon, L. Muzzi, N. Pompeo, R. Fastampa, M. Giura, S. Sarti, M. Boffa, A. M. Cucolo, M.C. Cucolo, *Physica C* **404**, 350 (2004)

⁴⁰ E. Silva, invited talk at the “European Workshop on Nanostructured Superconductors: from fundamentals to applications”, May 15-19, 2004, Bad Münstereifel (Germany); E. Silva et al., unpublished

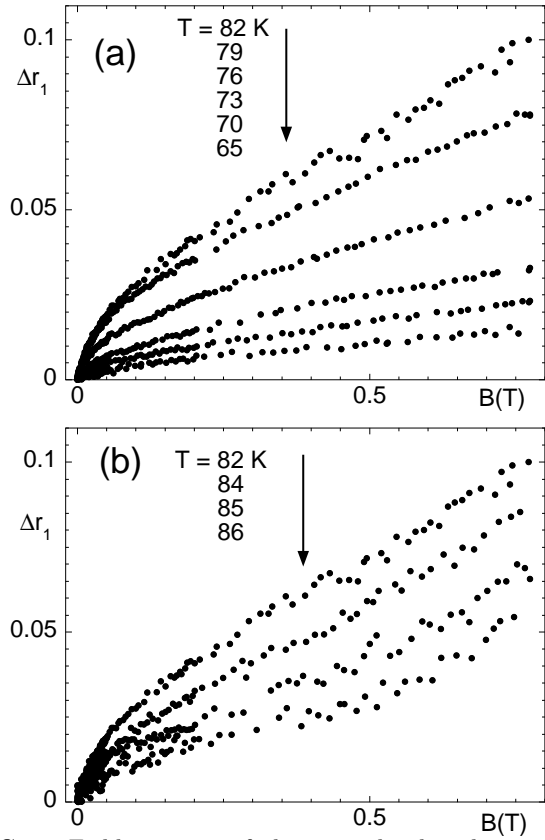


FIG. 1. Field increase of the normalized real microwave resistivity Δr_1 in sample A at 48.2 GHz at selected temperatures. Upper panel: raise of Δr_1 with increasing temperature up to $T_{max} \sim 82$ K. Lower panel: the amplitude decreases above T_{max} .

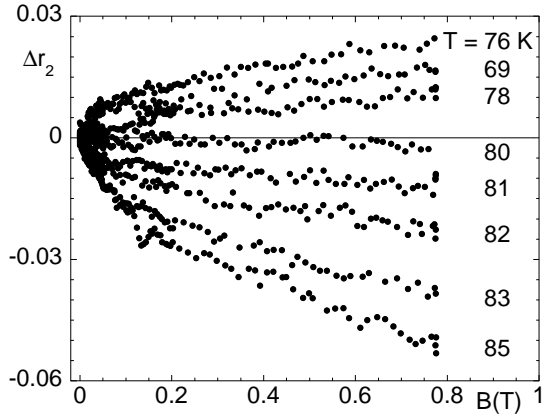


FIG. 2. Field variation of the normalized imaginary microwave resistivity Δr_2 in sample A at 48.2 GHz at selected temperatures. Up to $T_0 \sim 80$ K the field variation is positive, above T_0 it becomes negative.

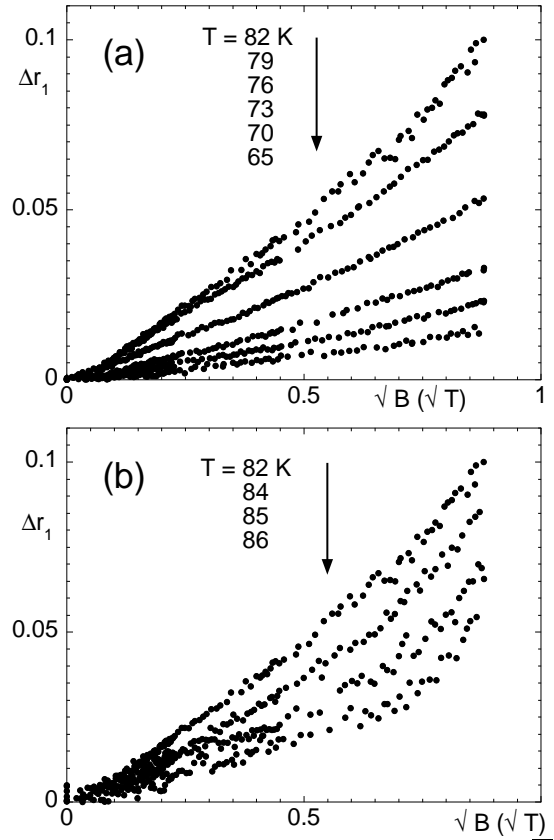


FIG. 3. Same data as in Figure 1, plotted against \sqrt{B} . The data show a detectable upward curvature.

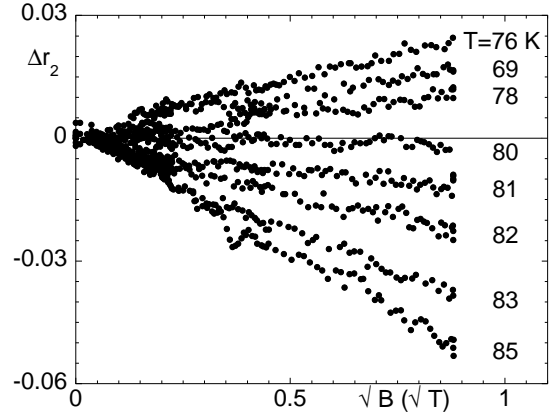


FIG. 4. Same data as in Figure 2, plotted against \sqrt{B} . The data exhibit a nearly perfect linear behaviour.

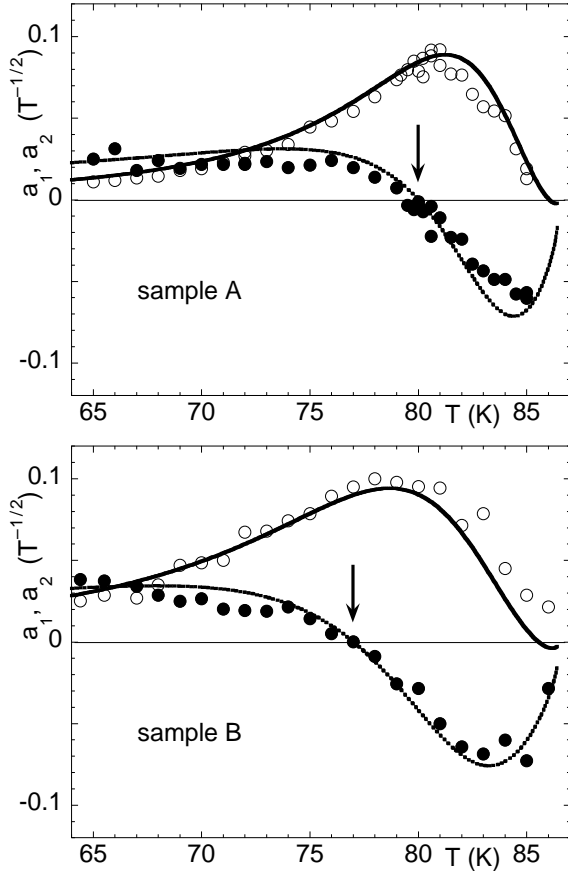


FIG. 5. Temperature dependence of the coefficients of the \sqrt{B} terms in the real (a_1) and imaginary (a_2) parts of the normalized resistivity. Open symbols: a_1 , full symbols: a_2 . Arrows mark the temperature T_0 where the imaginary resistivity is nearly insensitive to the applied field. Upper panel: sample A; lower panel: sample B. Continuous and dashed lines are the simultaneous fits with Equations 9 and 10, respectively. For each pair of fits only an overall scale factor is used.

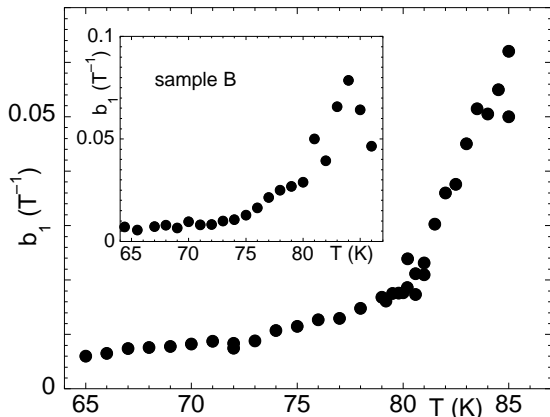


FIG. 6. Temperature dependence of the coefficients b_1 of the $\sim B$ term in the real part of the normalized resistivity, related to the vortex contribution. Main panel, sample A. Inset, sample B.

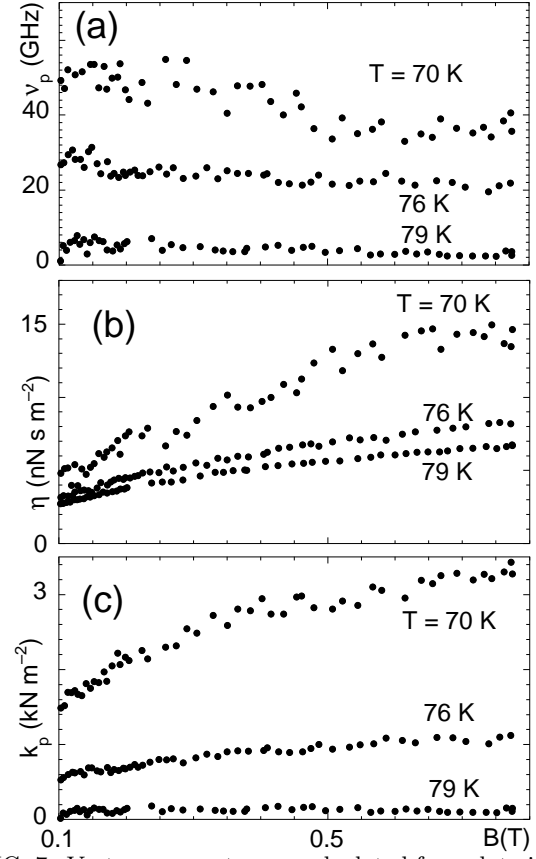


FIG. 7. Vortex parameters as calculated from data in sample A according to the conventional Gittleman-Rosenblum model. (a): pinning frequency. (b): vortex viscosity. (c): pinning constant. The strong field dependence of the so-calculated vortex viscosity and pinning constant cannot be easily justified.

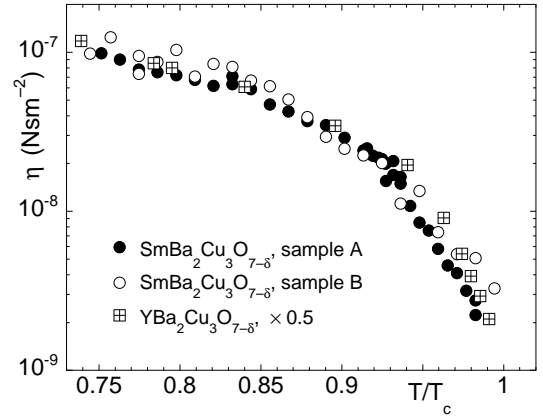


FIG. 8. Vortex viscosity in SmBCO (full dots, sample A; open circles, sample B) and in YBCO (squares) as a function of the reduced temperature. Data in YBCO are scaled by a factor 2 to show the collapse on the same curve as in SmBCO. Critical temperatures are $T_c = 86.5$ K in SmBCO samples, and $T_c = 89.3$ K in YBCO. The viscosity in SmBCO is the same in both samples. The temperature dependence is identical in YBCO and SmBCO.